CAVITATION INCEPTION IN FAST STARTUP

S. Duplaa[1] , O. Coutier-Delgosha[1], A. Dazin[1], G. Bois[2], G. Caignaert[3], O. Roussette[4]

Arts et Métiers ParisTech / LML Laboratory, 8 boulevard Louis XIV, 59046 Lille cedex, France
[1](0033)320622167, [2](0033)320622223, [3](0033) 320622221, [4](0033) 320620983
sebastien.duplaa@lille.ensam.fr, olivier.coutier@lille.ensam.fr, antoine.dazin@lille.ensam.fr,
gerard.bois@lille.ensam.fr, guy.caignaert@lille.ensam.fr, roussette@ensam.fr

ABSTRACT

The start-up of rocket engine turbopumps is generally performed only in a few seconds. It implies that these pumps reach their nominal operating conditions after only a few rotations. During these first rotations of the blades, the flow evolution in the pump is governed by transient phenomena, based mainly on the flow rate and rotation speed evolution. These phenomena progressively become negligible when the steady behaviour is reached. The pump transient behaviour induces significant pressure fluctuations which may result in partial flow vaporization, i.e. cavitation. An existing experimental test rig has been updated in the LML laboratory (Lille, France) for the start-ups of a centrifugal pump. The study focuses on cavitation induced during the pump start-up. Instantaneous measurement of torque, mass flow rate, inlet and outlet unsteady pressures, and pump rotation velocity enable to characterize the pump behaviour during rapid starting periods.

NOMENCLATURE

b	height of the blade to blade channels	(m)
C_u	tangential component of the velocity	(m/s)
C_r	radial component of the velocity	(m/s)
C	torque	(Nm)
I_{fluide}	Fluid inertia moment	(kgm^2)
I_p	Shaft inertia moment	(kgm^2)
K	$= \omega_f \times T_{na} / \Phi_{nf}$	(-)
P_s	static pressure in the pump suction pipe	(Pa)
Pd	static pressure in the pump delivery pipe	(Pa)
P_{vs}	vapor pressure	(Pa)
Q	volume flow rate	(m^3/s)
r	impeller radius	(m)
S	limit of the fluid volume in the channels	(m^2)
t	time	(s)
T_{na}	time to reach 63.2% of ω_f	(s)
u	tip velocity $=\omega \times r$	(m/s)
v	$Q / (2\pi r_2 b)$	(m/s)
β	relative flow angle	(-)
ΔP	pump head	(Pa)
χ	torque coefficient $= C / \rho\omega^2 r_2^5$	(-)
δ	flow rate coefficient : $= Q / u_2 r_2^2$	(-)
ϕ	ratio $C_r / C_u = Q / 2\pi r_2 b u_2$	(-)
Ψ	pressure coefficient $= \Delta P / \rho u_2^2$	(-)
η	pump efficiency	(-)
ω	rotation speed	(s^{-1})
ω_s	specific speed	(-)
σ	cavitation number $= (P_s - P_{vs})/(½\ \rho u_2^2)$	(-)
τ	$= (P_s + ½\rho v^2 - P_{vs})/(½\ \rho u_2^2)$	(-)
ρ	density	(kg/m^3)

Indices:

f	final (steady part of the fast start up)
n	nominal
1	pump inlet
2	pump outlet
hyd	hydraulic
nf	non cavitating final condition
st	steady
tr	transient
max	maximum value

INTRODUCTION

Space launcher turbopumps are characterized by fast start-ups: actually, the time delay between the inception of the shaft rotation and the nominal flow conditions is usually close to one second. It means that the rotation speed increases from zero up to several tens of thousands of rotations per minute during a single second. Such fast start-up results in severe transient effects that are mainly governed by the speed acceleration $d\omega / dt$ and the flow rate increase dQ / dt [1].

Transient effects in centrifugal pumps have been studied experimentally by several means for about 25

years: fast opening or closure of valves [2], fast start-up and shutdown sequences [3, 4, 5, 6], and /or rotation speed fluctuations [7]. It has been found in these previous studies that fast transients result in pronounced unsteady effects involving large pressure and mass flow rate fluctuations, which may be preponderant in front of the quasi – steady flow evolution. So, the understanding and the prediction of these transient behaviors is of first importance for the design of the feed pumps of rocket engines.

For this purpose, an experimental setup has been developed in the LML laboratory. It is presently devoted to the study of a five blades centrifugal runner. An original start-up sequence based on the use of a rapid coupling is applied in order to simulate rocket engine fast startings and the associated transient effects. Non-cavitating conditions have been previously investigated [5, 6] and the evolution of global parameters of the flow during the start-up (flow rate, pump head, pump rotation speed) has been obtained for various flow conditions. Local investigations have also been performed by Picavet and Barrand [5] in order to characterize the flow at the pump suction. A strong tangential velocity has been detected by visualizations at the pump inlet. PIV measurements performed in the inlet pipe have confirmed the presence of this recirculation, whose length and intensity have been characterized according to the final rotation speed and mass flow rate [6].

These previous investigations have been mainly conducted in non-cavitating flow conditions. However, pressure fluctuations involved in pump fast start-ups may be responsible for the development of cavitation in the impeller and in the inlet pipe. Indeed, cavitation is a recurrent source of perturbation for pumps operating at low inlet pressure and/or high rotation speed. Such conditions may be encountered during fast start-ups. Tanaka and Tsukamoto [2] have studied the transient flow in a centrifugal pump during fast start-up or shut down sequence: they have found strong fluctuations of both the mass flow rates and the pressures at inlet and outlet. While some of these fluctuations, which occur simultaneously at pump suction and delivery, are attributed by the authors to water hammer phenomenon, other oscillations, only detected at pump outlet, are due to unsteady cavitation. According to the measurements reported in [2], such oscillations depend both on the value of the cavitation number σ and on the mass flow rate.

The objective of the present study is to analyze this transient cavitating behavior in order to characterize the influence of low inlet pressure on fast start-ups of pumps. For this purpose, the test rig has been updated so that the instantaneous torque can be measured and an initial flow circulation can be imposed before the pump start-up.

1. EXPERIMENTAL DEVICE

The test rig has been initially constructed in 1993 for the study of fast start-up of centrifugal pumps. It has been used since that time for the investigation of fast transients in various situations of non-cavitating flows.[8, 9, 10].

For the purpose of the present study, the set-up has been significantly modified in order to improve its capabilities of measurement and also to enable different types of initial conditions.

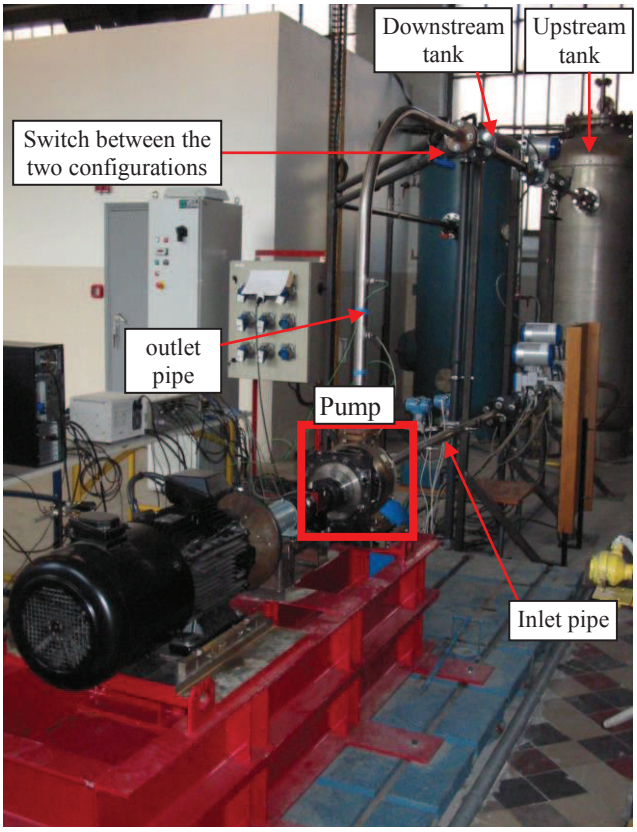

Figure 1. General view of the test rig

Two different configurations are available (figure 1):

- configuration #1: suction pipes and delivery pipes of the pump are connected to a single tank, so that the test rig is closed. In this situation, the flow velocity in the rig before the pump start-up is zero.
- configuration #2: delivery pipes are connected to a second tank, which means that the inlet and outlet initial pressures can be set independently. It enables to impose an initial flow circulation before the pump start up.

The switch between the two configurations is controlled with a valve located on the pump delivery pipe (figure 1).

In order to achieve fast starting periods, a special conception of the line of shafts is required: the pump is driven by an asynchronous electric motor through an electromagnetic clutch. The fast start-ups are obtained by engaging the clutch, once the motor is running at its final

rotation speed. Slower start-ups can also be obtained by engaging the clutch before the motor is started.

A single stage vaneless diffuser single volute type radial flow pump is used for the experiments. The main specifications of the impeller are summarized in Table 1 and figure 2.

Several high frequency measurements are available on the installation, in order to characterize the flow evolution during the pump fast start-up:

- A Meiri 0170MS torquemeter is included between the pump and the electromagnetic clutch in order to obtain the instantaneous rotation speed and torque.

- Four Kistler 701A piezoelectric pressure transducers are located on the inlet and delivery pipes. Their signals are used to obtain as well the high frequency inlet and outlet pressure evolutions as the inlet and outlet flow rates, according to the method initially proposed by Ghelici [6].

- The motor shaft rotation speed is measured by a photoelectric cell.

- An accelerometer located on the pump casing is used to obtain the radials vibrations.

Moreover, supplementary low frequency instrumentation is also available in order to control the final flow conditions after the transients or to characterize stabilized flow conditions. For this purpose, two Krohne Optiflux 4300 flow meters are used for the mass flow rate control at the pump suction and delivery, and two Rosemount pressure sensors are devoted to the measurements of the inlet pressure and pump head, respectively.

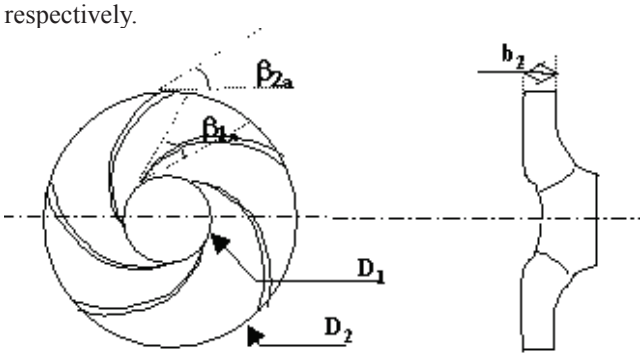

Figure 2: Impeller geometry
(a) Schematic view (b) picture

Geometric specifications		Hydraulic parameters	
Inlet vane angle	32.2°	ω_n	2900 rpm
Outlet vane angle	23°	Q_n	23 m^3/h
Number of vanes	5	ΔP_n	4.9 bar
Inlet diameter D_1	38.5 mm		
Outer diameter D_2	202.5 mm		
Outer width b_2	7 mm		

Table 1: Impeller specifications

The high frequency data from the pressure transducers and the torquemeter are acquired by a National Instrument PXI-PCI system equipped for the simultaneous acquisition of all signals. The sampling frequency is 10 kHz, and the acquisition duration is 5s. In the case of fast start-ups, acquisition is triggered by a TTL signal emitted at the engagement of the electromagnetic clutch, so that all experiments have the same reference time.

For steady state flow conditions, the uncertainty on the measurements has been evaluated from both the precision of the sensors and repeatability tests. In non-cavitating conditions and a rotation speed equal to 3000 rpm, the overall relative uncertainty is 5% for the torque, 1% for the unsteady pressure measurements, 0.5% for the inlet pressure and the pump head, and 4% for the mass flow rate, respectively. In cavitating conditions, uncertainty on torque and unsteady pressure increases up to 6.5% and 2%, respectively.

For transient flow conditions, the absolute uncertainties obtained from repeatability tests are reported in table 2, as well for cavitating as non cavitating conditions. The final rotation speed is always 3000 rpm. Note that absolute uncertainties are given for both steady (st) and transient (tr) situations. It can be seen that the precision of the measurements may decrease slightly during fast start-ups. The value 45 rpm reported for the rotation speed in transient flow conditions is mainly due to a random time delay in the rotation speed increase, which is related to the variable slipping of the electromagnetic clutch when it is engaged.

	P_s (bar)		P_d (bar)		C (Nm)		ω (rpm)	
	st	tr	st	tr	st	tr	st	tr
No cavitation	0.015	0.03	0.02	0.11	0.15	0.5	0	45
cavitation	0.015	0.015	0.06	0.1	0.5	0.5	0	45

Table 2: absolute uncertainties derived from repeatability tests (steady /transient conditions, with /without cavitation)

2. STEADY FLOW MEASUREMENTS

The behavior of the impeller has first been characterized in configurations of stabilized flow rates and rotation speeds in non-cavitating and cavitating conditions.

2.1 Non cavitating behavior

The evolution of the pump head according to the mass flow rate is given in figure 3 for three different rotation speeds. The nominal flow rate Q_n is defined as the conditions leading to zero incidence at the blade leading edge. The corresponding flow rate coefficient is 0.021. Mass flow rates have been investigated from 0.13 Q_n up to 1.5 Q_n. To obtain charts drawn in figure 3, non-cavitating conditions have been imposed by increasing the pressure level in the tank up to 3 bar.

It can be observed in figure 3 that a close agreement between the three results is obtained. Only a slight decrease of the pump head can be observed at rotation speed 1000 rpm, in comparison with the two other speeds. It shows that for rotation speeds ranging from 1000 to 3000 rpm, the non-cavitating flow in the pumps matches a similarity law.

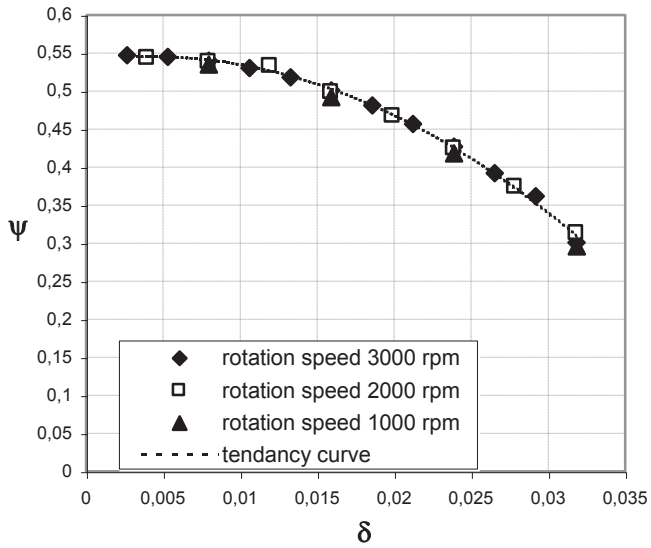

Figure 3: Evolution of the pump elevation according to the flow rate coefficient

Figures 4a and 4b show the evolutions of the torque and the efficiency according to the flow rate coefficient. Note that the efficiency of the whole pump including the volute is considered here. The variation of χ as a function of the dimensionless rotation speed ω/ω_n is given in figure 4c. It can be observed that for rotation speeds higher than 1200 rpm (ω/ω_n = 0.4) a nice similarity is obtained, while for small rotation speeds, the torque increases significantly. This poor similarity at low speed is confirmed in figure 4d, which shows the evolution of the amplitude of radial vibrations on the pump caasing according to the flow coefficient for three rotation speeds.

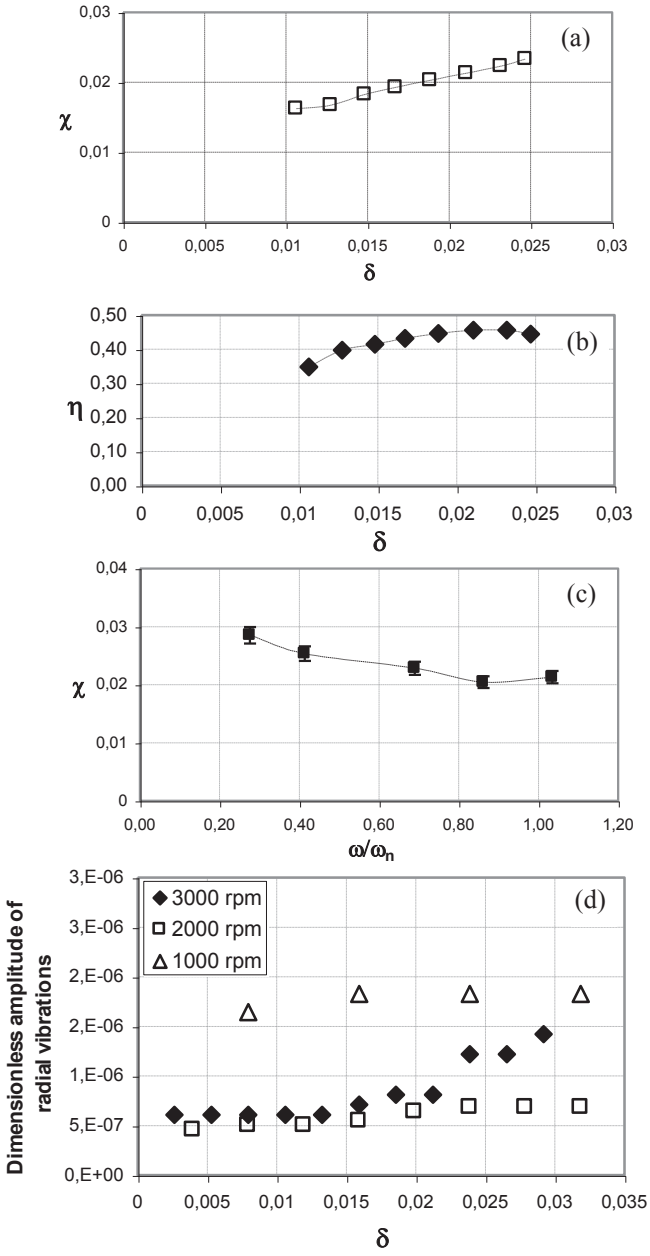

Figure 4: Evolution of (a) χ, (b) η according to δ, (c) χ according to ω/ω_n, (d) the dimensionless amplitude of the radial vibrations according to δ

2.2 Cavitating behavior

The effects of cavitation on the pump performance have been studied first in steady flow conditions: the head drop charts have been obtained at several rotation speeds and several values of the flow coefficient, by progressively decreasing the pressure in the tank. Only rotation speeds 2500 rpm and 3000 rpm have been investigated, so that at least 20% pressure drop can be obtained. A close

agreement between dimensionless charts obtained at both speeds is obtained in figure 5. It shows that similarity laws can be extended to cavitating behavior at such speeds.

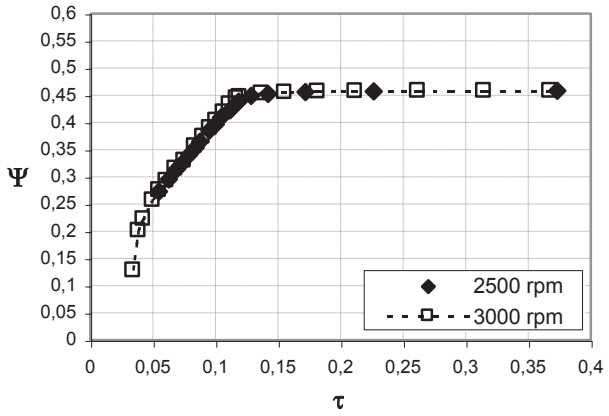

Figure 5: Head drop charts at 2500 and 3000 rpm (nominal flow rate)

Figure 6 displays the cavitating behavior of the pump at 3000 rpm for several flow rates. Although the pump geometry leads to a quite small value of $\omega_s = 0.24$, the decrease of the pump elevation is progressive at all flow rates. Figure 7 shows the evolution of the values of τ corresponding to 3%, 10%, and 20% head drop, respectively, according to the flow rate. Nearly identical slopes are obtained for the three curves, which demonstrates a similar pump behavior at all flow rates.

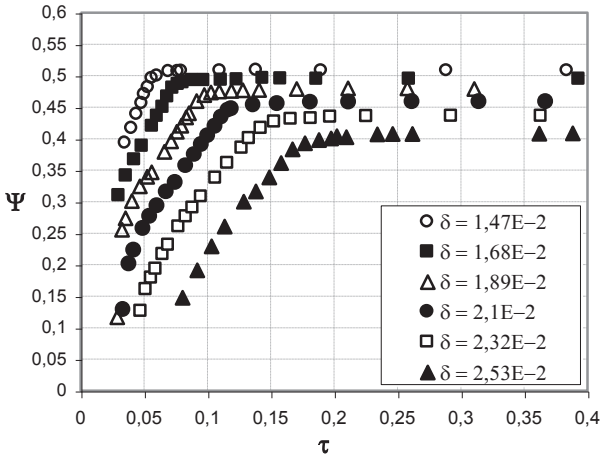

Figure 6: Head drop charts for six flow rates at 3000 rpm

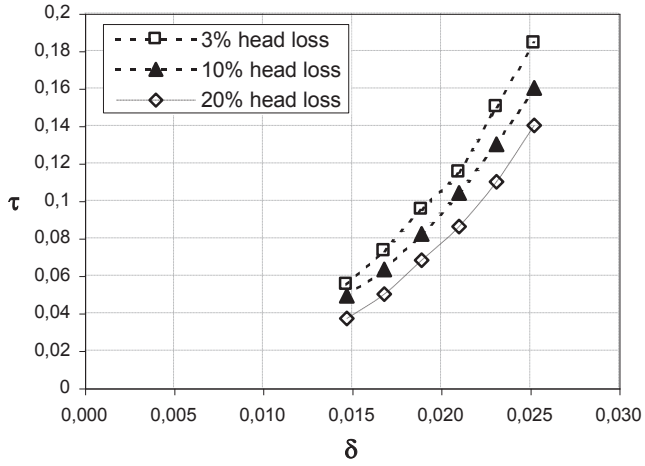

Figure 7: Evolution of τ according to δ for 3%, 10% and 20% head drop (3000 rpm)

Figure 8 shows the decrease of the pump head according to the flow rate for constant values of the cavitation number σ. The curve corresponding to non-cavitating flow conditions is also drawn in order to visualize the head drop due to cavitation. It can be observed that the head drop increases with the flow rate. It suggests that cavitation occurs also on the pressure side of the blades when the flow rate is increased up over the nominal value $\delta_n = 0.021$. This pressure side cavity leads to a local inversion of the pressure difference on both sides of the blades, which progressively deteriorates the pump elevation. However, figure 9 shows that the efficiency also decreases at high flow rate coefficient, which indicates that the pressure side cavity leads to a significant obstruction of the flow in the blade to blade channels. It induces also a progressive decrease of the flow coefficient corresponding to the optimal efficiency.

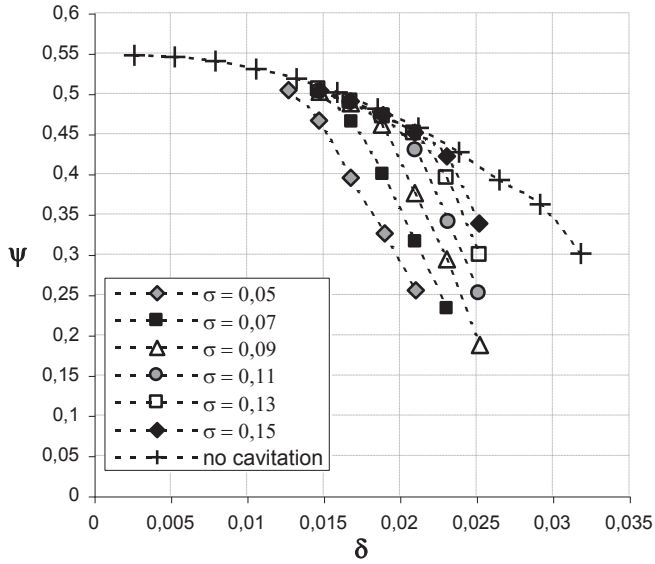

Figure 8: Evolution of the head drop according to δ at constant value of σ

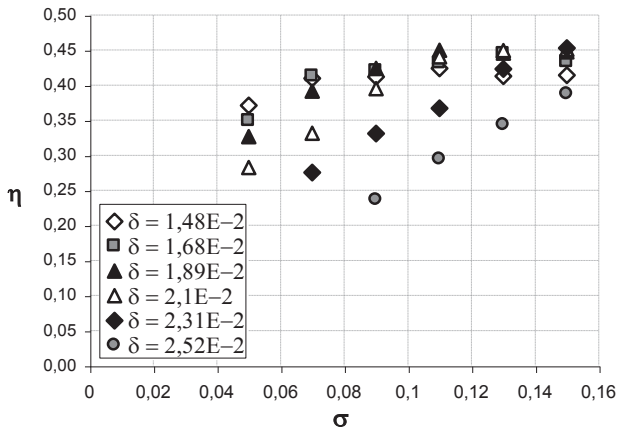

Figure 9: Evolution of the efficiency according to σ for six values of the flow rate coefficient (3000 rpm)

3. FAST START-UPS

Transient behaviors have been also investigated by performing fast start-ups of the pump at several flow rates in non-cavitating and cavitating conditions.

3.1 Non cavitating conditions

The high frequency signals resulting from a fast start-up performed at nominal flow rate are displayed in figures 10 to 12. The time evolutions of the pressure at suction (P_s) and delivery (P_d) are drawn in figure 10, together with the pump head (P_d-P_s). The start-up itself corresponds to the first 0.45s, while the second part of the signals is related to steady flow conditions that are obtained at the end of the starting period. This is confirmed by figure 11, which shows the evolution of the rotation speed as a function of time. The pressure decrease in the pump suction pipe (blue curve) is related to the unsteady effects associated with flow rate and rotation speed variations.

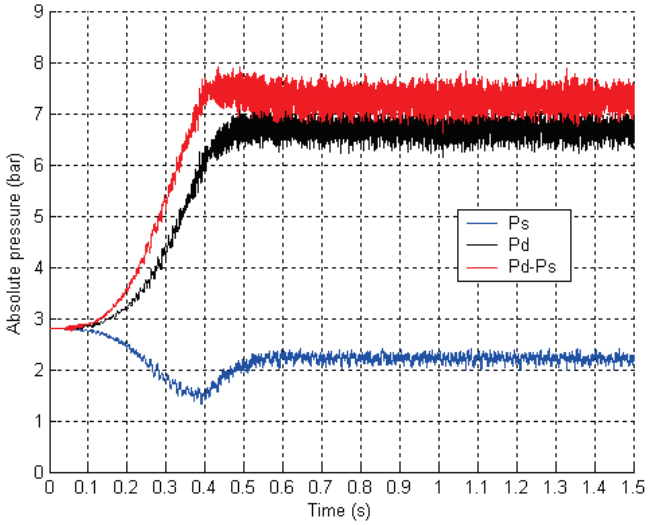

Figure 10: Evolution of the pump head and of the pressure at inlet and outlet of the pump ($Q_f = Q_n$, $\omega_f = 3000$ rpm)

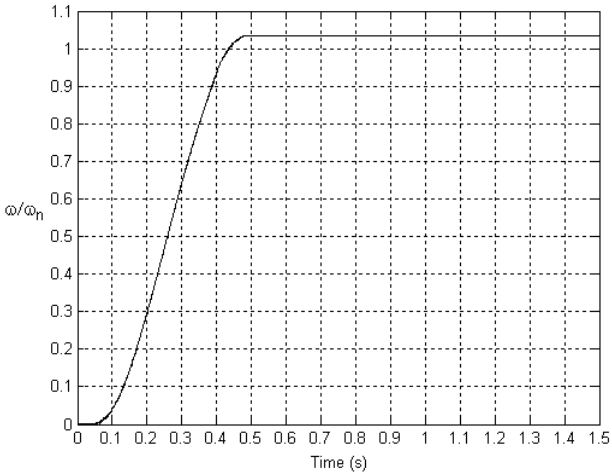

Figure 11: Evolution of the rotation speed ($Q_f = Q_n$, $\omega_f = 3000$ rpm)

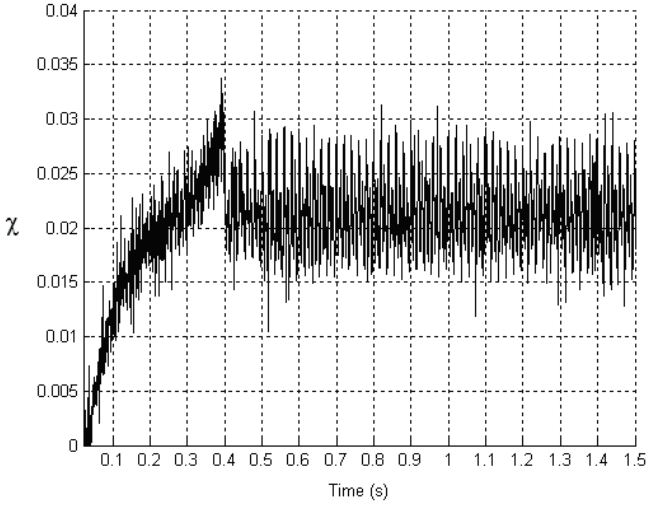

Figure 12: Evolution of the dimensionless torque ($Q_f = Q_n$, $\omega_f = 3000$ rpm)

The torque evolution is shown in figure 12. Periodical fluctuations at frequency of the pump rotation (50 Hz) are obtained in steady flow conditions. To investigate the peak that occurs at the end of the start-up, the expression of the torque is given hereafter (Dazin et al., 2007 [1]):

$$C = \iint_S \rho r c_u c_r ds + (I_{fluide} + I_p)\frac{\partial}{\partial t}(\omega) - (\rho \int_h^R \frac{r}{\tan\beta} dr)\frac{\partial}{\partial t} Q_v$$

The first term on the right hand side is identical to the one obtained in steady flow conditions: it corresponds to the increase of the moment of momentum in the pump. Conversely, terms 2 and 3 are due to the unsteady flow evolution: term 2 is related to the inertial moment of the fluid (I_{fluide}) and the shaft (I_p) when the impeller is accelerated, while term 3 is due to the flow rate variations in the pump. This equation is solved numerically on the basis of the evolutions of ω and Q measured in the experiment. The comparison between the numerical result

and the torque measured during the start-up is displayed in figure 13.

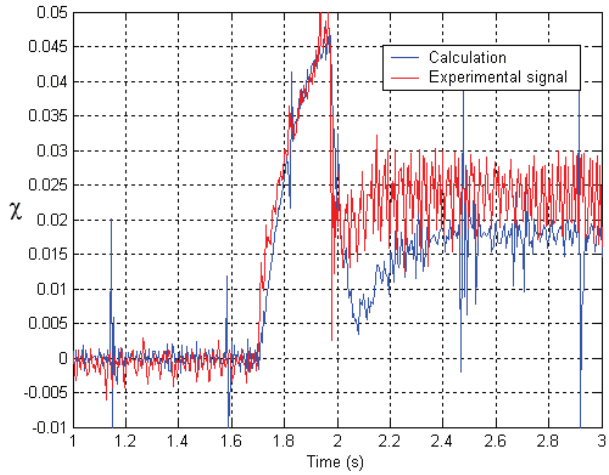

Figure 13: comparison between the measured and calculated dimensionless torque ($Q_f = Q_n$, $\omega_f = 2000$ rpm)

Although some discrepancies can be observed concerning the prediction of the steady-flow torque magnitude, a reliable agreement is obtained regarding the peak amplitude and shape.

Since the torque peak occurs for high values of $d\omega/dt$ (see figures 10 and 11), it is expected that the ratio C_{max} / C_{st} (where C_{max} denotes the maximum torque value and C_{st} is the torque value in steady flow conditions) depends mainly on the fluid and solid inertia. I_p is estimated to be much higher than I_{fluide}, so C_{max} / C_{dest} may be close to the following expression:

$$\frac{C_{max}}{C_{st}} \approx \frac{C_{st} + I_p \frac{\partial \omega}{\partial t}}{C_{st}} = 1 + \frac{I_p \frac{\partial \omega}{\partial t}}{C_{st}}$$

This expression is calculated numerically and compared to the experimental values of C_{max} / C_{st} for several rotation speeds, at nominal flow rate (figure 14).

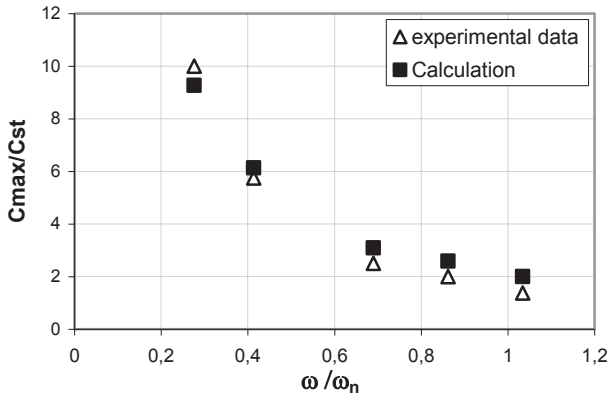

Figure 14: Comparison between the measured and calculated values of C_{max} / C_{st} ($Q_f = Q_n$)

A close agreement between the experimental data and the calculated values is obtained for all rotation speeds. It confirms than the shaft inertia is mainly responsible for the torque peak observed at the end of the fast start-ups.

3.2 Cavitating conditions

When the pressure in the tank is decreased so that cavitation is obtained during the transient or even in steady flow conditions, three types of pressure signals displayed in figures 15 to 17 are obtained. All data are obtained for a final rotation speed equal to 3000 rpm, since it was shown previously in Section 2.2 that behaviours at other rotation speeds could be derived from a single one by similarity laws.

Tests have been conducted for various values of flow rate and cavitation number. In most of the cases, pressure signals evolutions similar to the one drawn in figure 15 (denoted hereafter "case 1") are obtained. In comparison with non cavitating situations (see figure 10), the pressure at pump suction, after the initial fall, remains completely stable during most of the start-up ($0.25s < t < 0.45s$). Its magnitude during this period is slightly higher than the vapour pressure. This behaviour indicates that cavitation occurs in the pump inlet pipe and /or inside the pump. The pressure at delivery is characterized by a significant drop at the end of the start-up, which may be related to the temporary decrease of the pump head because of cavitation on the blades. The delivery signal also exhibits high frequency fluctuations whose maximum amplitude is about 50% of the pump head. This may be due to vapour collapse at the pump outlet.

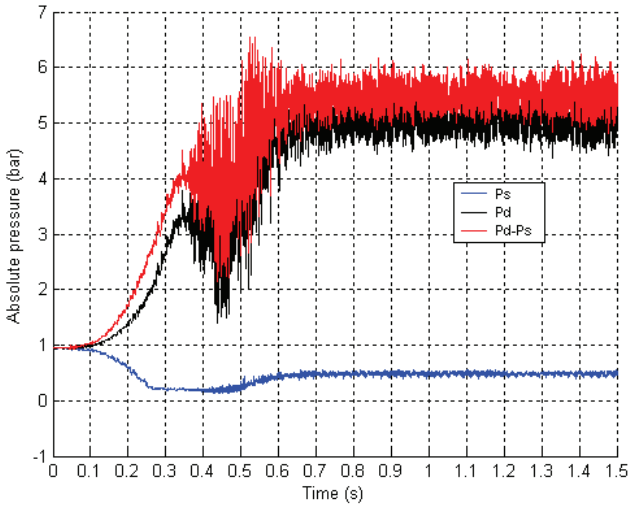

Figure 15: Evolution of the pump head and of the pressure at inlet and outlet of the pump (case 1) ($\sigma = 0.09$, $Q_f = 0.9\ Q_n$, $\omega_f = 3000$ rpm)

These pressure fluctuations at the pump outlet can be associated with the drastic increase of the magnitude of the radial vibrations measured on the pump casing, in

comparison with non-cavitating conditions (figure 16). Note that the maximum amplitude of the vibrations is correlated with the maximum pressure fluctuations at the pump outlet (0.4s < t <0.5s).

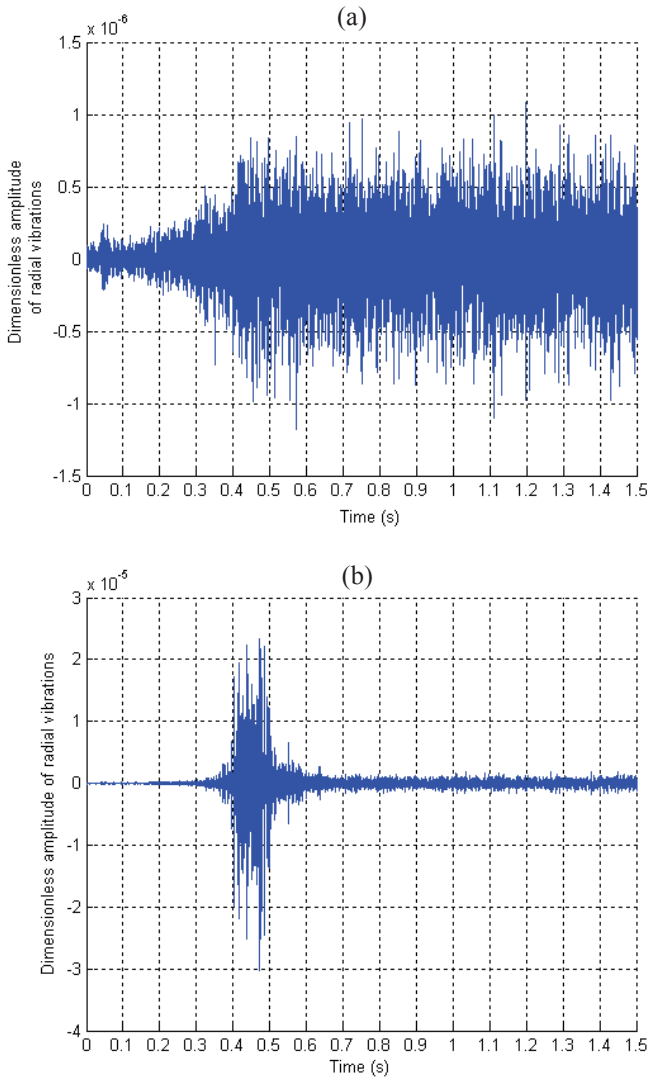

Figure 16: Amplitude of the radial vibrations on the pump casing for ω_f = 3000 rpm and Q = Q_n
(a) Non cavitating conditions, (b) σ = 0.09
(Different scales in ordinate)

For high flow rates (at least 1.1 Qn) slightly different pressure signals are obtained (figure 17). Low frequency oscillations of the delivery pressure can be observed at the end and after the transient period. This particular behaviour, denoted "case 2" hereafter, may be due to the obstruction generated by pressure side cavitation on the blades: such blockage results in a significant decrease of the pump head, as can be seen in figure 8 in steady state situations. Low amplitude pressure oscillations can also be observed on the inlet pressure signal, which suggests that this phenomenon is related to a surge type instability that affects the whole pump.

A third typical pattern of the pressure signals is obtained for intermediate values of the cavitation number and lower flow rates. In such conditions of moderate cavitation, a pressure peak is obtained at the pump suction at the end of the transient (figure 18). Note that a peak of similar magnitude occurs also at the same time at delivery, although it is not so visible because of high frequency pressure fluctuations. Such simultaneous pressure jumps can be associated with a water hammer phenomenon, as it was previously stated by Tanaka et al. [3].

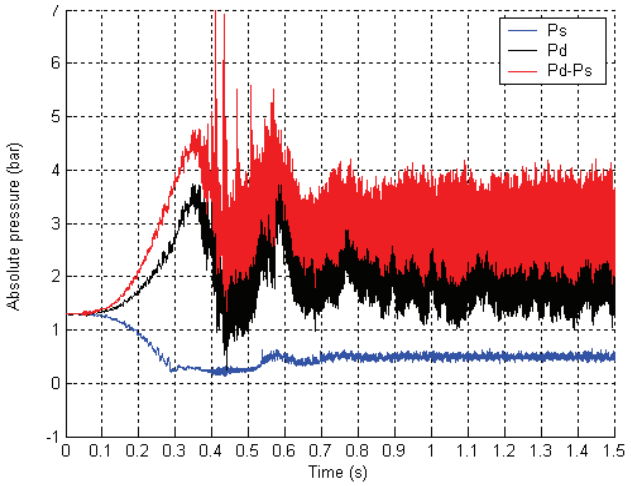

Figure 17: Evolution of the pump head and of the pressure at inlet and outlet of the pump (case 2)
(σ = 0.09, Q_f = 1.2 Q_n, ω_f = 3000 rpm)

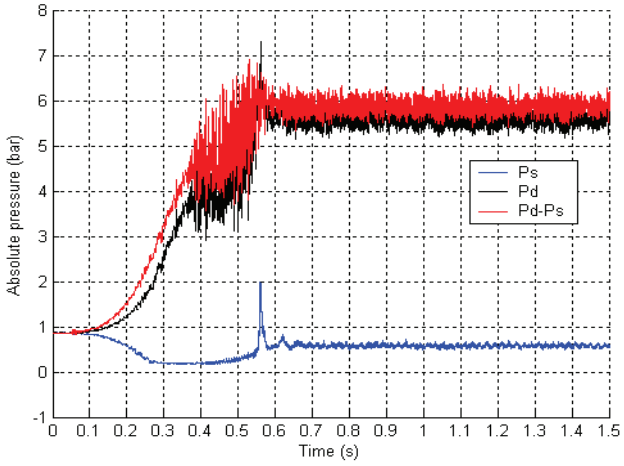

Figure 18: Evolution of the pump head and of the pressure at inlet and outlet of the pump (case 3)
(σ = 0.11, Q_f = 0.7 Q_n, ω_f = 3000 rpm)

The whole tests performed in cavitating conditions have been classified into these three different categories of transients, and the resulting map is drawn in figure 19. It

confirms that large scale oscillations systematically occur at high flow rate and in conditions of developed cavitation, while water hammer phenomena are detected at lower flow rate and for a moderate development of cavitation. Such a classification has been proposed previously by Tanaka et al. [3], whereas these authors have investigated a quite different range of σ and δ (figure 20a, b). Note that the parameter K used in ordinate is based on a characteristic time of the start-up T_{na}, the final rotation speed N_f, and a flow rate coefficient ϕ_{nf}. $N_f \times T_{na}$ characterises how fast the start up is, while ϕ_{nf} is related to the final flow rate in steady state conditions. The present experiments are reported in the same diagram (figure 20b) in order to enable the comparison with the data reported in [3].

Tanaka et al. have also detected two types of cavitation behaviors:

- one denoted "no fluctuation" that exhibits only a drop of the delivery pressure at the end of the start-up
- a second one denoted "oscillating cavitation", which is obtained at large flow coefficient and low cavitation number: it involves low frequency fluctuations both at the pump inlet and outlet.

Note that in both situations, no high frequency fluctuation is reported by the authors.

So, case 1 (figure 15) in the present experiments seems very close to the situation denoted "no fluctuation" in [3], and case 2 (figure 17), which is obtained also at large flow rates and low cavitation numbers, is similar to the situation of "oscillating cavitation" reported in [3].

It can be observed (figure 20) that the present tests correspond to an area of the diagram that was not investigated by Tanaka et al. However, the few data common to both sets of results ($\sigma \approx 0.013$) exhibit as well water hammer situations (case 3) as cavitation oscillations belonging to cases 1 and 2. It suggests that the limit between cavitation oscillations and water hammer phenomena may be not so obvious as the one proposed in [3] (see figure 20a). As a matter of facts, parameters used to classify the different tests (K and σ_f) may be inadequate to separate ours different types of results.

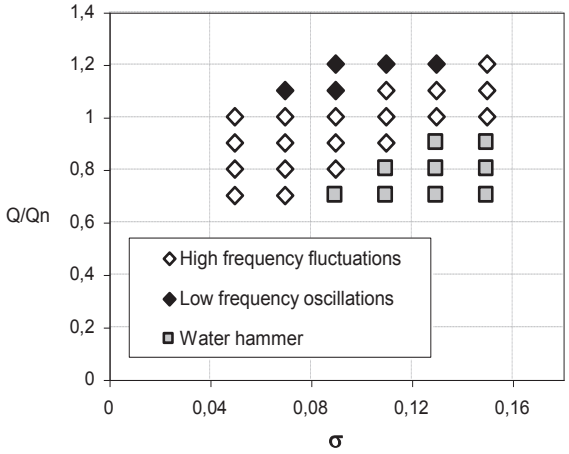

Figure 19: classification of the start-ups

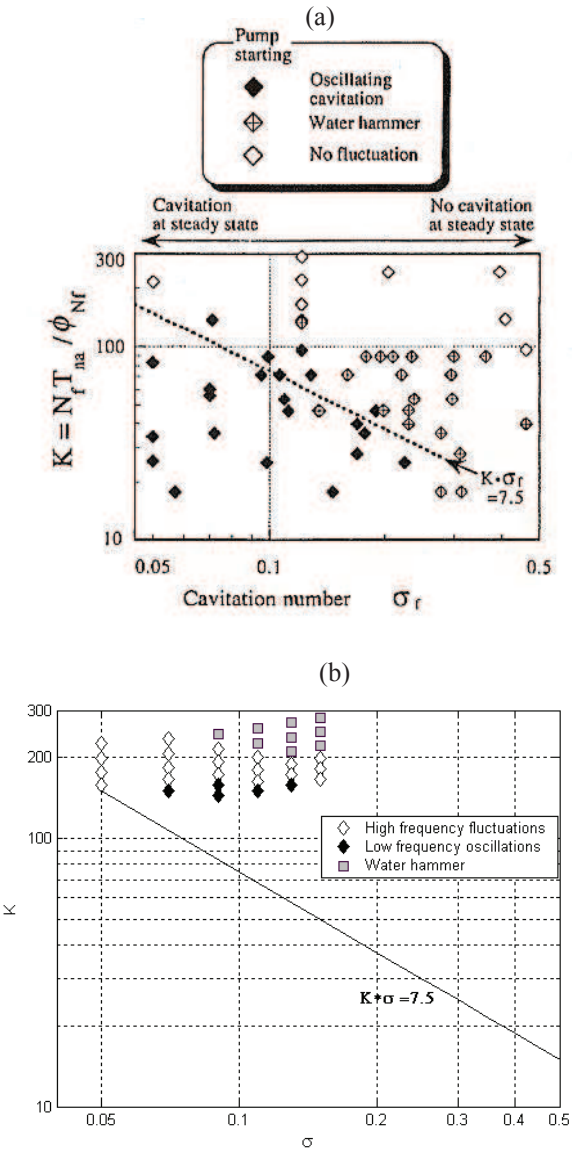

Figure 20: comparison between the present set of data and the previous results reported in [3]
(a) Data from Tanaka et al., (b) present experiments

CONCLUSION

The behavior of a centrifugal pump has been studied in cavitating and non cavitating conditions. Both steady state flow situations and fast start-ups have been investigated. The effects of cavitation on the pump head at constant rotation speed has been characterized. Different types of unsteady behaviors have been obtained during the transients performed in cavitating conditions. At high flow rate, low frequency oscillations of large amplitude are obtained on the pressure signal at delivery (case 2), whereas at lower flow rate, only a drop at the end of the start-up is detected (case 1). At moderate cavitation number and low flow rate, water hammer phenomena are also observed.

These results are consistent with the previous data reported by Tanaka et al. [3] with a similar impeller geometry. Adequate parameters to classify the different transient cavitating situations have still to be determined. Local non-intrusive measurements inside the impellers will be performed in the LML research team, in order to characterize more precisely the cavitation pattern obtained in the different cases detected presently.

ACKNOWLEDGEMENTS

The present work was performed in the scope of a research grant from the CNES (French Space Agency) and SNECMA Moteurs.

The authors wish to express their gratitude to SNECMA Moteurs and the CNES for their continuous support.

The authors also express their gratitude to the technical staff of the LML laboratory, especially J. Choquet and P. Olivier, who have been involved in the realisation of the test facility.

REFERENCES

[1] Dazin A., Caignaert G., Bois G., Experimental and theoretical analysis of a centrifugal pump during fast starting period. Journal of Fluids engineering, 129, 1436-1444, 2007

[2] Tanaka T., H. Tsukamoto, Transient behaviour of a cavitating centrifugal pump at rapid change in operating conditions—Part 1:Transient phenomena at opening / closure of discharge valve. Journal of Fluids Engineering, 121, 841-849, 1999.

[3] Tanaka T., H. Tsukamoto, Transient behaviour of a cavitating centrifugal pump at rapid change in operating conditions—Part 2: Transient phenomena at pump Start-up/Shutdown. Journal of Fluids Engineering, 121, 850-856, 1999.

[4] Tanaka T., H. Tsukamoto, Transient behaviour of a cavitating centrifugal pump at rapid change in operating conditions—Part 3: Classifications of transient phenomena. Journal of Fluids Engineering, 121, 857-865, 1999

[5] Picavet A., Barrand J.P., Fast start-up of a centrifugal pump – Experimental study. Pump congress, Karlsruhe, 1996.

[6] Bolpaire S., Barrand J.P., Caignaert G., Experimental study of the flow in the suction pipe of a centrifugal pump impeller : steady conditions compared with fast start-up. International Journal of Rotating Machinery, 8(3) : 215-222, 2002.

[7] Lefebvre P.J., Barker W.P., Centrifugal Pump Performance During Transient Operation, Journal of Fluids Engineering, March 1995, vol. 117, pp 123 – 128

[8] Ghelici N., Etude du régime transitoire de démarrage rapide d'une pompe centrifuge, PhD Thesis. Ecole Nationale Supérieure d'Arts et Métiers, September 1993.

[9] Picavet A., Etude des phénomènes hydrauliques transitoires lors du démarrage rapide d'une pompe centrifuge, PhD Thesis. Ecole Nationale Supérieure d'Arts et Métiers. 1996

[10]. Bolpaire S. : Etude des écoulements instationnaires dans une pompe en régime de démarrage ou en régime établi. PhD Thesis. Ecole Nationale Supérieure des Arts et Métiers. 2000.